Formation and activation energy of $Cd_xZn_{1-x}Te$ nanostructures with different dimensions grown on ZnTe buffer layers

Cite as: Appl. Phys. Lett. **88**, 043111 (2006); https://doi.org/10.1063/1.2168244
Submitted: 27 April 2005 • Accepted: 01 December 2005 • Published Online: 26 January 2006

T. W. Kim, H. S. Lee and H. L. Park

Formation and activation energy of $Cd_xZn_{1-x}Te$ nanostructures with different dimensions grown on ZnTe buffer layers

T. W. Kim[a)]
Research Institute of Information Display, Division of Electronics and Computer Engineering, Hanyang University, 17 Haengdang-dong, Seongdong-gu, Seoul 133-791, Korea

H. S. Lee and H. L. Park
Institute of Physics and Applied Physics, Yonsei University, Seoul 120-749, Korea

(Received 27 April 2005; accepted 1 December 2005; published online 26 January 2006)

Atomic force microscopy (AFM) and photoluminescence (PL) measurements were carried out to investigate the formation process and the activation energy of different-dimensional $Cd_xZn_{1-x}Te/ZnTe$ nanostructures. The results of the AFM images show that $Cd_xZn_{1-x}Te$ quantum dots (QDs) are formed and that the dimensional transformation from $Cd_xZn_{1-x}Te$ QDs to $Cd_xZn_{1-x}Te$ quantum wires is caused by coalescence. The excitonic peak corresponding to the transition from the ground electronic subband to the ground heavy-hole transitions in $Cd_xZn_{1-x}Te/ZnTe$ nanostructures shifts to lower energy with increasing thickness of the $Cd_xZn_{1-x}Te$ layer due to variations in the thickness and the dimension of the layer. The activation energy of the electrons confined in the $Cd_xZn_{1-x}Te/ZnTe$ nanostructures, as obtained from the temperature-dependent PL spectra, was significantly affected by the thickness and the dimension of the $Cd_xZn_{1-x}Te$ layer. © *2006 American Institute of Physics*. [DOI: 10.1063/1.2168244]

Promising applications of nanostructures in next-generation electronic and optoelectronic devices have driven extensive efforts to form various kinds of nanostructures on semiconductor substrates.[1–5] Among the various kinds of nanostructures, III–V/III–V nanostructures based on InAs/GaAs quantum dots (QDs), which are referred to as artificial atoms, have been the most extensively studied systems because of interest in both investigations of fundamental physical properties[6,7] and potential applications in electronic and optoelectronic devices, such as single-electron transistors,[8] QD lasers,[9] and QD infrared photodetectors.[10] Recently, II–VI/II–VI nanostructures based on wide-energy band gap II–VI compound semiconductors have attracted much attention because of their many potential applications for optoelectronic devices operating in the short-wavelength region.[10–12] However, relatively little work has been performed on II–VI/II–VI nanostructures in comparison with III–V/III–V nanostructures because of the delicate problems encountered in the growth process.[13–15] Among these II–VI/II–VI nanostructures, $Cd_xZn_{1-x}Te/ZnTe$ nanostructure systems have become particularly attractive because of their potential applications in optoelectronic devices operating in the green region of the spectrum.[16–18] Even though some studies concerning CdTe/ZnTe nanostructures consisting of binary compound semiconductors have been performed,[19,20] the formation and the optical properties of $Cd_xZn_{1-x}Te/ZnTe$ nanostructures have not yet been studied. Furthermore, $Cd_xZn_{1-x}Te/ZnTe$ layers have emerged as excellent candidates for possible fabrication of ferroelectric nonvolatile flash memories.[21]

Different-dimensional $Cd_xZn_{1-x}Te$ nanostructures were deposited on ZnTe buffer layers. Atomic force microscopy (AFM) measurements were performed to characterize the surface microstructural properties of $Cd_xZn_{1-x}Te$ layers of various thicknesses grown on ZnTe buffer layers. Photoluminescence (PL) measurements were carried out in order to investigate the interband transitions and to determine the activation energies in $Cd_xZn_{1-x}Te$ layers of various thicknesses embedded in ZnTe buffer layers acting as buffers.

The several kinds of samples used in this study were grown on semi-insulating (100)-oriented GaAs substrates by using molecular beam epitaxy (MBE) and consisted of the following structures: a 900 nm undoped ZnTe capping layer deposited by MBE, $Cd_xZn_{1-x}Te$ layers [1.5, 3.0, 4.5, 6.0, and 7.5 monolayers (MLs)] deposited by MBE, and a 100 nm undoped ZnTe buffer layer deposited by MBE. The depositions of the ZnTe and the $Cd_xZn_{1-x}Te$ layers were done at a substrate temperature of 320 °C, which is calibrated surface temperature. The source temperatures of the Cd, Zn, and Te sources for the $Cd_xZn_{1-x}Te$ layers were 220, 280, and 300 °C, respectively. The deposition of the $Cd_xZn_{1-x}Te$ layer was done at a system pressure of approximately 2.8×10^{-8} Torr.

Figure 1 show AFM images of the uncapped surfaces of the $Cd_{0.6}Zn_{0.4}Te$ layers deposited with thicknesses of (a) 1.5, (b) 3.0, (c) 4.5, (d) 6.0, and (e) 7.5 MLs on ZnTe buffer layers. When the thickness of the $Cd_{0.6}Zn_{0.4}Te$ layer is 1.5 ML, small-sized $Cd_{0.6}Zn_{0.4}Te$ QDs are formed on the ZnTe buffer layers, as shown in Fig. 1(a). The size of the $Cd_{0.6}Zn_{0.4}Te$ QDs increases with increasing thickness of the $Cd_{0.6}Zn_{0.4}Te$ layer, and the sizes becomes uniform, as shown in Fig. 1(b). However, when the thickness of the $Cd_{0.6}Zn_{0.4}Te$ layer is 4.5 ML, some of the $Cd_{0.6}Zn_{0.4}Te$ QDs start to coalesce on the ZnTe buffer layer and form $Cd_{0.6}Zn_{0.4}Te$ quantum wires, as shown in Fig. 1(c). When the thickness of the $Cd_{0.6}Zn_{0.4}Te$ layer is 6.0 ML, more of the $Cd_{0.6}Zn_{0.4}Te$ QDs coalesce, as shown in Fig. 1(d). However, when the thickness of the $Cd_{0.6}Zn_{0.4}Te$ layers is 7.5 ML, the QDs transform into quantum wires due to the coalescence, as shown in Fig. 1(e). After the thickness of the $Cd_{0.6}Zn_{0.4}Te$ layers is above 3.0 ML, a preferential growth direction ap-

[a)]Author to whom correspondence should be addressed; electronic mail: twk@hanyang.ac.kr

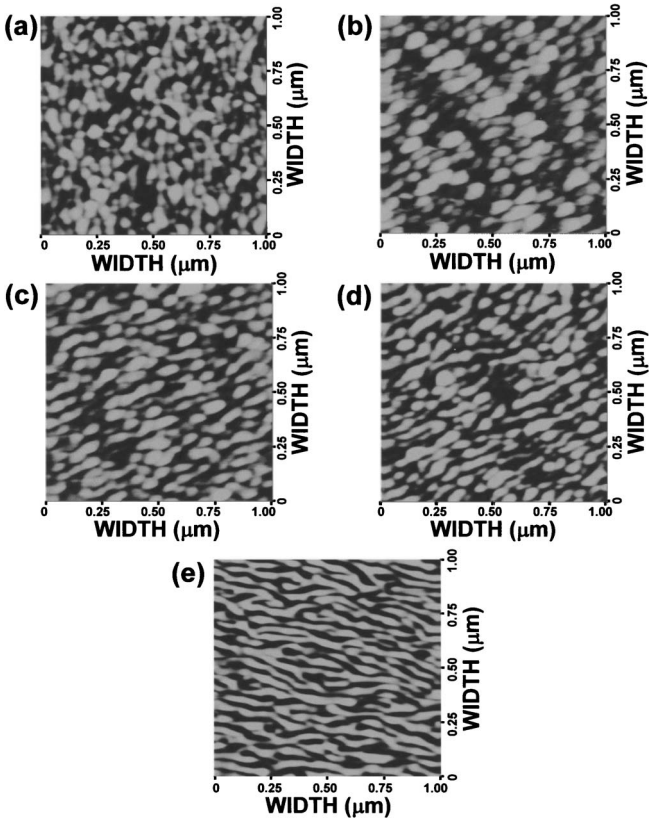

FIG. 1. Atomic force microscopy images of $Cd_{0.6}Zn_{0.4}Te$ layers with thicknesses of (a) 1.5, (b) 3.0, (c) 4.5, (d) 6.0, and (e) 7.5 MLs grown on ZnTe buffer layers.

pears in the $Cd_{0.6}Zn_{0.4}Te$ nanostructures. The shapes of the quantum wires have particular directions. The densities, the heights, and the diameters for various $Cd_{0.6}Zn_{0.4}Te$ layer thicknesses are summarized in Table I. The data show that a dimensional growth-mode transition gradually appears in the sample with a 4.5-ML-thick $Cd_{0.6}Zn_{0.4}Te$ layer, which is attributed to the formation of quantum wires, resulting from the coalescence of QDs, as shown in Fig. 1(c). The formation process of the $Cd_xZn_{1-x}Te$ quantum wires and the dimensional transition from the $Cd_xZn_{1-x}Te$ QDs to the quantum wires are similar to those for CdTe/ZnTe nanostructures.[19]

Figure 2 shows the PL spectra at 20 K for the $Cd_{0.6}Zn_{0.4}Te$ nanostructures with thicknesses of 1.5, 3.0, 4.5, 6.0, and 7.5 MLs. The peak corresponding to the exciton transition from the ground-state electronic subband to the ground-state heavy-hole band (E_1-HH_1) shifts to lower energy with increasing thickness of the $Cd_{0.6}Zn_{0.4}Te$ layer. This observed redshift of the PL peak position for the 4.5- and the 6.0-ML-thick nanostructures is attributed to a decrease in the quantum confinement effect, resulting from the transition of many QDs to quantum wires. The redshift behavior of the PL peak position for the 6.0- and 7.5-ML-thick nanostructures is

TABLE I. Densities, heights, and diameters for various $Cd_{0.6}Zn_{0.4}Te$ layer thicknesses.

CdTe layer thickness (mL)	Density (cm^{-2})	Height (nm)	Diameter (nm)
1.5	2×10^{10}	10	35–45
3.0	4×10^{10}	10	45–55
4.5	6×10^{10}	11	50–55

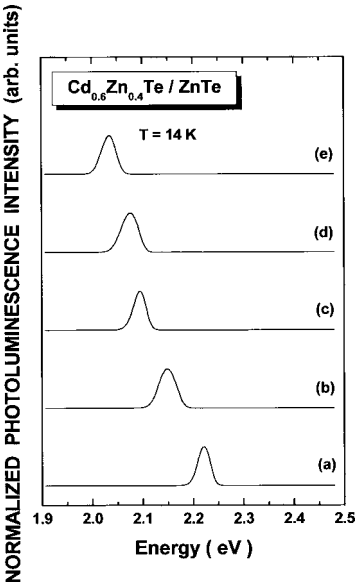

FIG. 2. Photoluminescence spectra at 14 K for $Cd_{0.6}Zn_{0.4}Te$ layers with thicknesses of (a) 1.5, (b) 3.0, (c) 4.5, (d) 6.0, and (e) 7.5 MLs grown on ZnTe buffer layers.

caused by decreasing energy difference between the ground-state electronic subband and the ground-state heavy hole, resulting from increasing number and width of $Cd_{0.6}Zn_{0.4}Te$ quantum wires.

In order to determine the activation energy of the electrons confined in the $Cd_{0.6}Zn_{0.4}Te$/ZnTe nanostructures, we performed temperature-dependent PL measurements. The results for the PL spectra measured at several temperatures for the $Cd_{0.6}Zn_{0.4}Te$/ZnTe nanostructures in 3.0- and 7.5-ML-thick $Cd_{0.6}Zn_{0.4}Te$ layers are shown in Fig. 3. Since the energy gaps of the $Cd_{0.6}Zn_{0.4}Te$ nanostructures decrease with increasing temperature, the PL peaks corresponding to the (E_1-HH_1), transitions shift to lower energy with increasing temperature. As the temperature is increased, the integrated PL intensity corresponding to the bound electron peak is given by[22]

$$I = I_0/[1 + C\ \exp(-\Delta E_A/k_BT)], \tag{1}$$

where I_0 is the integrated PL intensity at 0 K, C is the ratio of the thermal escape rate to the radiation combination rate,

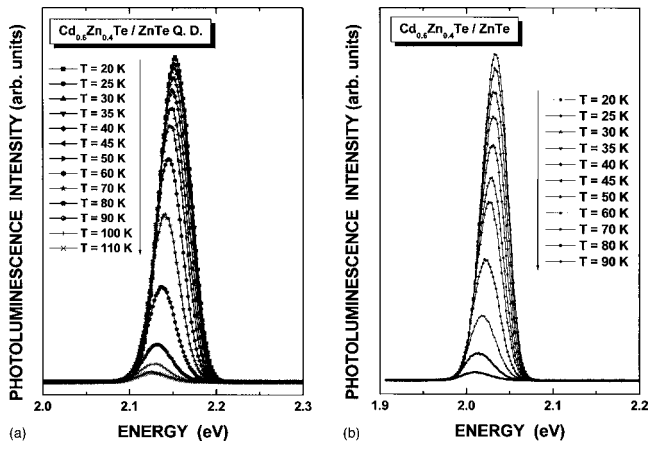

FIG. 3. Photoluminescence spectra at several temperatures for $Cd_{0.6}Zn_{0.4}Te$ quantum dots with thicknesses of (a) 3.0 and (b) 7.5 MLs grown on ZnTe buffer layers.

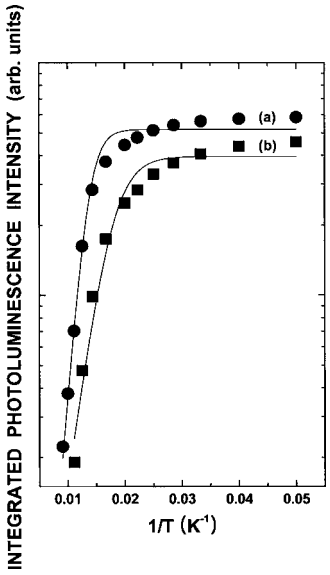

FIG. 4. Integrated photoluminescence intensities as functions of the reciprocal temperature for $Cd_{0.6}Zn_{0.4}Te$ nanostructures with thicknesses of (a) 3.0 and (b) 7.5 MLs grown on ZnTe buffer layers. The solid circles and rectangles represent the data for $Cd_{0.6}Zn_{0.4}Te$ nanostructures with thicknesses 3.0 and 7.5 MLs, respectively, and the dashed and the solid lines indicate the fitting curves.

ΔE_A is the activation energy, and k_B is the Boltzmann constant. From Eq. (1), the activation energies, ΔE_A, of the electrons confined in $Cd_{0.6}Zn_{0.4}Te/ZnTe$ nanostructures with 3.0 and 7.5 MLs, as determined from the solid lines of Fig. 4, are 60 and 35 meV, respectively. The activation energies of the electrons confined in $Cd_{0.6}Zn_{0.4}Te/ZnTe$ nanostructures are summarized in Table II. While the activation energy of the electrons confined in the nanostructures increases up to a $Cd_{0.6}Zn_{0.4}Te$ layer thickness of 3.0 ML, it decreases above 3.0 ML. Since the most uniform $Cd_{0.6}Zn_{0.4}Te$ QDs were formed in the 3.0-ML-thick $Cd_{0.6}Zn_{0.4}Te$ layer grown on a ZnTe buffer layer, the activation energy of the electrons confined in the 3.0-ML-thick $Cd_{0.6}Zn_{0.4}Te$ layer had the highest value among those observed for the various nanostructures investigated in this research. The much higher activation energy for the 3.0-ML-thick $Cd_{0.6}Zn_{0.4}Te$ layer originates from a uniformity enhancement of the QDs or from a reduction in the quantum dimension of the nanostructures, which is a consequence of an increase in the Coulomb interaction due to carrier confinement.[23,24]

In summary, $Cd_xZn_{1-x}Te/ZnTe$ nanostructures were grown by using MBE. AFM images showed that uniformly sized $Cd_xZn_{1-x}Te/ZnTe$ QDs were formed at a layer thickness of 3.0 ML and that as the thickness was increased further above 3.0 ML, a gradual transformation from $Cd_xZn_{1-x}Te/ZnTe$ QDs to $Cd_xZn_{1-x}Te/ZnTe$ quantum wire occurred due to coalescence. The peak position of the $(E_1\text{-}HH_1)$ excitonic transitions in the $Cd_xZn_{1-x}Te/ZnTe$ QDs shifted to lower energies with increasing thickness of the $Cd_xZn_{1-x}Te$ layer. The activation energy of the electrons confined in the 3.0-ML-thick $Cd_xZn_{1-x}Te$ QDs, as obtained from the temperature-dependent PL spectra, was higher than those of electrons confined in $Cd_xZn_{1-x}Te/ZnTe$ nanostructures with different thicknesses, and its value was as high as 60 meV. These present observations can help to improve understanding of the dimensional transition of the quantum confinement in $Cd_xZn_{1-x}Te/ZnTe$ nanostructures.

TABLE II. Activation energies and errors for various $Cd_{0.6}Zn_{0.4}Te$ layer thicknesses.

$Cd_{0.6}Zn_{0.4}Te$ layer thickness (ML)	Activation energy (meV)
1.5	50±1.5
3.0	60±2.0
4.5	50±1.5
6.0	45±1.3
7.5	35±1.2

This work was supported by the Korea Research Foundation Grant (KRF-2004-005-D00166).

[1] D. Leonard, M. Krishnamurthy, C. M. Reaves, S. P. Denbaars, and P. M. Petroff, Appl. Phys. Lett. **63**, 3203 (1993).
[2] S. A. Empedocles and M. G. Bawendi, Science **278**, 2114 (1997).
[3] R. Nötzel, Z. Niu, M. Ramsteiner, H-P. Schönherr, A. Tranpert, L. Däweritz, and K. H. Ploog, Nature (London) **392**, 56 (1998).
[4] R. J. Warburton, C. Schöflen, D. Haft, F. Bickel, A. Lorke, K. Karrai, J. M. Garcia, W. Schoenfeld, and P. M. Petroff, Nature (London) **405**, 926 (2000).
[5] M. Jung, K. Hirakawa, Y. Kawaguchi, S. Komiyama, S. Ishida, and Y. Arakawa, Appl. Phys. Lett. **86**, 033107 (2005).
[6] Y. Toda, O. Moriwaki, M. Nichioka, and Y. Arawaka, Phys. Rev. Lett. **82**, 4114 (1999).
[7] W. G. Van der Wiel, S. De Franceschi, J. M. Elzerman, S. Tarucha, L. P. Kouwenhoven, J. Motohisa, F. Nakajima, and T. Fukui, Phys. Rev. Lett. **88**, 126803 (2002).
[8] H. Cao, J. Y. Xu, W. H. Xiang, Y. Ma, S. H. Chang, S. T. Ho, and G. S. Solomon, Appl. Phys. Lett. **76**, 3519 (2000).
[9] I. N. Kaiander, R. L. Sellin, T. Kettler, N. N. Ledentsov, D. Bimberg, N. D. Zakharov, and P. Werner, Appl. Phys. Lett. **84**, 2992 (2004).
[10] E.-T. Kim, A. Madhukar, Z. Ye, and J. C. Campbell, Appl. Phys. Lett. **84**, 3277 (2004).
[11] X. Y. Kong, Y. Ding, R. Yang, and Z. L. Wang, Science **303**, 1348 (2004).
[12] K. A. Alim, V. A. Fonoberov, and A. A. Balandin, Appl. Phys. Lett. **86**, 053103 (2005).
[13] H. Kirmse, R. Schneider, M. Rabe, W. Neumann, and F. Henneberger, Appl. Phys. Lett. **72**, 1329 (1998).
[14] G. Karczewski, S. Maćkowski, M. Kutrowski, T. Wojtowicz, and J. Kossut, Appl. Phys. Lett. **74**, 3011 (1999).
[15] T. W. Kim, E. H. Lee, K. H. Lee, J. S. Kim, and H. L. Park, Appl. Phys. Lett. **84**, 595 (2004).
[16] T. W. Kim, K. H. Lee, and H. L. Park, Appl. Phys. Lett. **72**, 563 (1998).
[17] H. S. Lee, H. L. Park, and T. W. Kim, Appl. Phys. Lett. **85**, 5598 (2004).
[18] S. Mackowski, T. Gurung, H. E. Jackson, L. M. Smith, W. Heiss, J. Kossut, and G. Karczewski, Appl. Phys. Lett. **86**, 103101 (2005).
[19] T. W. Kim, D. C. Choo, D. U. Lee, H. S. Lee, M. S. Jang, and H. L. Park, Appl. Phys. Lett. **81**, 487 (2002).
[20] S. Mackowski, H. E. Jackson, L. M. Smith, W. Heiss, J. Kossut, and G. Karczewski, Appl. Phys. Lett. **83**, 254 (2003).
[21] D. J. Fu, J. C. Lee, S. W. Choi, S. J. Lee, T. W. Kang, M. S. Jang, H. I. Lee, and Y. D. Woo, Appl. Phys. Lett. **81**, 5207 (2002).
[22] See, for example, E. W. Williams and H. B. Bebb, in *Semiconductors and Semimetals*, edited by R. K. Willardson and A. C. Beer (Academic, New York, 1992), Vol. 8, p. 321.
[23] D. Birkedal, J. Singh, V. G. Lyssenko, J. Erland, and J. M. Hvam, Phys. Rev. Lett. **76**, 672 (1996).
[24] R. C. Miller, D. A. Kleinman, A. C. Gossard, and O. Munteanu, Phys. Rev. B **25**, 6545 (1982).